Progress In Electromagnetics Research Letters, Vol. 23, 19–28, 2011

CHAOTIC BEHAVIOR IN RECEIVER FRONT-END LIMITERS

F. Caudron and A. Ouslimani

ECS Lab., EA3649, ENSEA
6 Av. du Ponceau, Cergy Cedex 95014, France

R. Vézinet

CEA, DAM, GRAMAT
Gramat F-46500, France

A. Kasbari

ECS Lab., EA3649, ENSEA
6 Av. du Ponceau, Cergy Cedex 95014, France

Abstract—A delay nonlinear differential equation is proposed to investigate the condition of the microwave chaotic behavior existing between the antenna and the front-end protection circuit of a receiver such as the radar front-end limiter circuit. This investigation concerns the case of intentional or unintentional signals applied to the antenna outside of its bandwidth. Bifurcation diagrams show that the chaotic behavior appears for antenna impedance up to 10 Ω and for amplitudes greater than 1.2 V. Electrical simulation results agree well with theoretical ones.

1. INTRODUCTION

Radar receivers necessitate sensitive front-end circuits such as low noise amplifiers or RF detectors to process very small signals. Front-end protection circuits such as limiters are often used to limit the level of intentional or unintentional electromagnetic interferences. Limiters are generally placed between the receive antenna and receiver circuits. Most of them use the PIN diodes as power controllers [1–3]. In nonlinear region and under certain conditions, the PIN diode can

Received 3 February 2011, Accepted 8 April 2011, Scheduled 12 April 2011
Corresponding author: François Caudron (francois.caudron@ensea.fr).

generate chaotic phenomena. Consequently due to a large chaos bandwidth, certain frequencies can affect the radar operation. The chaotic behavior has already been observed in a microwave limiter circuit [4], in 'R-L-Diode' circuits [5] and also in VHF microstrip oscillator [6]. Some theoretical approaches have been proposed for diode resonator [7, 8]. In this paper, we present a theoretical study in order to understand the origin of microwave chaotic behavior in front-end RF limiter circuits. A delay nonlinear differential equation is derived from this study. This equation allows us to investigate the conditions in which the chaotic behavior can appear. Microwave electrical simulations are used to validate the theoretical study.

2. THEORY

Figure 1 presents the studied front-end limiter structure. It's a limiter circuit model with a PIN diode-terminated transmission line.

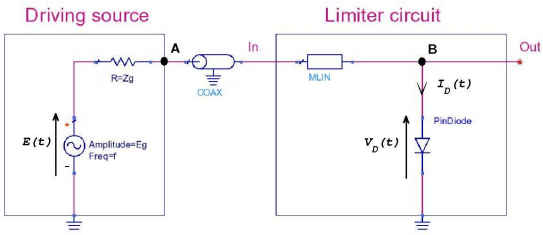

Figure 1. Limiter structure and the driving source, "COAX" coaxial transmission line and "MLIN" microstrip transmission line.

For radar applications, the antenna can be described by a driving sinusoidal source $E(t)$ with the amplitude E_g and the impedance Z_g:

$$E(t) = E_g \cos(2\pi f t + \varphi_0) \tag{1}$$

with f, the frequency and φ_0, the initial value of the phase.

We consider that these two transmission lines "COAX" and "MLIN" are lossless. We also consider that the coaxial microstrip transition doesn't affect the characteristic impedance Z_0. In this case, we have a single line without losses and with a global delay time T_d. Diode current $I_D(t)$ and diode voltage $V_D(t)$ can be expressed as function of the incident voltage $V_+(t)$ and the reflected voltage $V_-(t)$ at the node "B" (Figure 1):

$$V_D(t) = V_+(t) + V_-(t) \tag{2}$$

$$Z_0 I_D(t) = V_+(t) - V_-(t) \tag{3}$$

By adding and subtracting the Equations (3) and (2), we obtain respectively (4a) and (4b):

$$2V_+(t) = V_D(t) + Z_0 I_D(t) \tag{4a}$$

and

$$2V_-(t) = V_D(t) - Z_0 I_D(t) \tag{4b}$$

The incident voltage $V_+(t)$ can be expressed using the delayed reflected voltage $V_-(t - 2\,T_d)$ and the delayed driving voltage $E(t - T_d)$:

$$V_+(t) = \Gamma(t - T_d)\, V_-(t - 2\,T_d) + \alpha(t - T_d)\, E(t - T_d) \tag{5}$$

The parameters $\Gamma(t)$ and $\alpha(t)$ represent respectively the reflection coefficient and transmission coefficient versus time at the node "A". A relation between $V_D(t)$, $I_D(t)$ and $E(t)$ can be derived from the Equations (4) and (5):

$$\begin{aligned} &V_D(t) - \Gamma(t - T_d) V_D(t - 2\,T_d) + Z_0\,(I_D(t) + \Gamma(t - T_d) I_D(t - 2\,T_d)) \\ &= 2\,\alpha(t - T_d)\, E(t - T_d) \end{aligned} \tag{6}$$

Using the PIN diode model shown in Figure 2, we can relate $V_D(t)$ and $I_D(t)$ (7) [9, 11, 12]:

$$I_D(t) = I(t) + \frac{d}{dt} q(t) \tag{7}$$

with

$$I(t) = I_s \left[\exp\left(\frac{V_D(t)}{\beta V_t} \right) - 1 \right] \tag{8}$$

where I_s is the diode saturation current, the voltage V_t is the thermal voltage and β is an ideality coefficient.

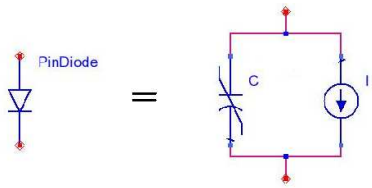

Figure 2. The equivalent electrical model of the PIN diode.

The depletion charge $q(t)$ is describe by the capacitor C [10, 11]:

$$q(t) = C_D(t)\, V_D(t) + \tau I_D(t) \tag{9}$$

where τ is the carrier lifetime and $C_D(t)$ is the capacitor defined as:

$$C_D(t) = \frac{C_{j0}}{\left(1 - \frac{V_D(t)}{V_0}\right)^{\frac{1}{2}}} \tag{10}$$

The capacitor C_{j0} is defined in the unbiased state and V_0 is the built-in potential.

The current $I_D(t)$ can be rewritten using the Equations (7) to (10):

$$I_D(t) = \left(1 + \tau \frac{d}{dt}\right) I(t) + C_{j0} V_0{}^{\frac{1}{2}} \frac{d}{dt} \frac{V_D(t)}{(V_0 - V_D(t))^{\frac{1}{2}}} \tag{11}$$

Equations (6) and (11) give the delay nonlinear differential equation:

$$\begin{aligned} & V_D(t) - \Gamma(t - T_d)\, V_D(t - 2\,T_d) \\ & + Z_0 \left(\left(1 + \tau \frac{d}{dt}\right) I(t) + C_{j0} V_0{}^{\frac{1}{2}} \frac{d}{dt} \frac{V_D(t)}{(V_0 - V_D(t))^{\frac{1}{2}}} \right. \\ & \left. + \Gamma(t - T_d) \left(\left(1 + \tau \frac{d}{dt}\right) I(t - 2\,T_d) + C_{j0} V_0{}^{\frac{1}{2}} \frac{d}{dt} \frac{V_D(t - 2\,T_d)}{(V_0 - V_D(t - 2\,T_d))^{\frac{1}{2}}} \right) \right) \\ & = 2\,\alpha(t - T_d)\, E(t - T_d) \end{aligned} \tag{12}$$

The transmission coefficient $\alpha(t)$ is determined as:

$$\alpha(t) = \frac{Z_0}{Z_0 + Z_g} \left(1 + \Gamma_D(t - T_d)\, \cos\left(2\pi f\, 2T_d\right)\right) \tag{13}$$

$\Gamma_D(t)$ is the reflection coefficient at the node "B". It is given by:

$$\Gamma_D(t) = \frac{\frac{V_D(t)}{I_D(t)} - Z_0}{\frac{V_D(t)}{I_D(t)} + Z_0} = \frac{V_D(t) - Z_0\, I_D(t)}{V_D(t) + Z_0\, I_D(t)} \tag{14}$$

The reflection coefficient $\Gamma(t)$ at the node "A" is determined using the Equation (15):

$$\Gamma(t) = \frac{Z_g - Z_0}{Z_g + Z_0} \tag{15}$$

The Equation (12) becomes:

$$\begin{aligned} & V_D(t) - \Gamma(t - T_d)\, V_D(t - 2\,T_d) \\ & + Z_0 \left(\left(1 + \tau \frac{d}{dt}\right) I(t) + C_{j0} V_0{}^{\frac{1}{2}} \frac{d}{dt} \frac{V_D(t)}{(V_0 - V_D(t))^{\frac{1}{2}}} \right. \\ & \left. + \Gamma(t - T_d) \left(\left(1 + \tau \frac{d}{dt}\right) I(t - 2\,T_d) + C_{j0} V_0{}^{\frac{1}{2}} \frac{d}{dt} \frac{V_D(t - 2\,T_d)}{(V_0 - V_D(t - 2\,T_d))^{\frac{1}{2}}} \right) \right) \\ & = 2\,\frac{Z_0}{Z_0 + Z_g} \left(1 + \frac{V_D(t - 2\,T_d) - Z_0\, I_D(t - 2\,T_d)}{V_D(t - 2\,T_d) + Z_0\, I_D(t - 2\,T_d)} \cos\left(2\pi f\, 2T_d\right)\right) \\ & E_g \cos\left(2\pi f (t - T_d) + \varphi_0\right) \end{aligned} \tag{16}$$

The delay nonlinear differential Equation (16) is solved using the Matlab® software.

The PIN diode is a commercial PIN diode "BAP64-02" [13] often used for designing RF attenuators and limiters applications up to 3 GHz. The parameters of the transmission line are $T_d = 1\,\text{ns}$ and $Z_0 = 50\,\Omega$. The initial phase value φ_0 of the driving source is taken equal to zero. Figure 3 shows the bifurcation diagrams calculated at $f = 1\,\text{GHz}$. The bifurcation diagrams present the local maxima of the voltage $V_D(t)$ versus the bifurcation parameters Z_g in Figure 3(a) and E_g in Figure 3(b). A finite integer number of local maxima corresponds to a periodic behavior ($Z_g > 10\,\Omega$ and $E_g < 1.2\,\text{V}$). A infinity of local maxima corresponds to a chaotic behavior. From these results, we can deduce that the chaotic behavior appears for important impedance mismatch up to $Z_g = 10\,\Omega$ and for a minimum driving voltage $E_g = 1.2\,\text{V}$. The important impedance mismatch added to the presence of a nonlinear component such as diodes working in the nonlinear region favor the chaos generation.

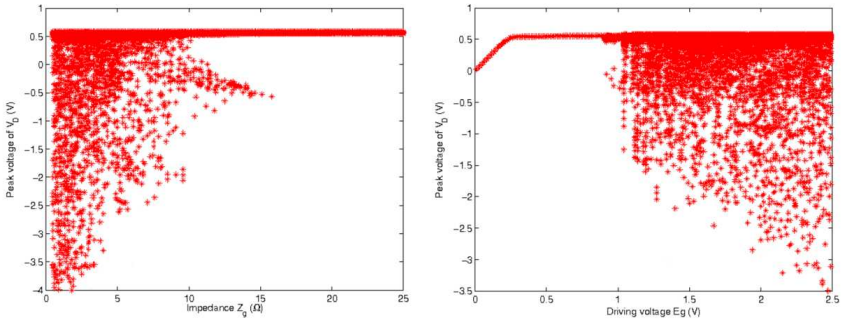

(a) (b)

Figure 3. Bifurcation diagrams: (a) Bifurcation parameter Z_g with $E_g = 2\,\text{V}$ and (b) bifurcation parameter E_g with $Z_g = 5\,\Omega$.

The method of induced electromotive force and the analytical expressions of the radiated and electrical powers allow to obtain an electrical model of a dipole antenna [14, 15]. Equations (17) give the resistance R_{dipole} and the reactance X_{dipole} of the radiation impedance for a dipole antenna:

$$R_{dipole} = \frac{\eta}{2\pi \sin^2(kl/2)} \left(C + \ln(kl) - Ci(kl) + \frac{1}{2}\sin(kl)(Si(2kl) - 2Si(kl)) \right.$$
$$\left. + \frac{1}{2}\cos(kl)\left(C + \ln\left(\frac{kl}{2}\right) + Ci(2kl) - 2Ci(kl) \right) \right) \qquad (17a)$$

and

$$X_{dipole} = \frac{\eta}{4\pi \sin^2(kl/2)} \left(2Si(kl) + \cos(kl)(2Si(kl) - Si(2kl)) - \sin(kl) \left(2Ci(kl) - Ci(2kl) - Ci\left(\frac{2ka^2}{l}\right)\right)\right) \quad (17b)$$

where Ci and Si are the cosine and sine integral functions, l is the dipole length, a is the dipole radius, $k = 2\pi f c^{-1}$ with $c = 3$ ($10^8\,\mathrm{ms}^{-1}$), $\eta = 120\pi\,\Omega$ (impedance in free space), $C = 0.577$. Figure 4 depicts R_{dipole} and X_{dipole} versus frequency.

For the frequencies outside the antenna bandwidth and more precisely for those lower than f_0, R_{dipole} is of few ohms and this leads to an impedance mismatch.

Figure 5 shows the bifurcation diagram using the parameter T_d. From Figure 5, the chaotic regime occurs every $T_d = 0.5\,\mathrm{ns}$. This is due to the periodicity of the term "$\cos(2\pi f 2T_d)$" in the expression of $\alpha(t)$ in Equation (16). This periodicity is equal to $T_d = f^{-1}/2 = 0.5\,\mathrm{ns}$ at 1 GHz. Figure 6 plots the attractors for different delay times T_d. The attractors display the voltage $V_D(t)$ versus the current $I_D(t)$.

For $T_d \in \{n\frac{T}{2};\ n \in \mathbb{N}^*\}$, the trajectory fills the phase space (Figure 6(b)). For all other values of T_d, the chaos phenomena is very reduced.

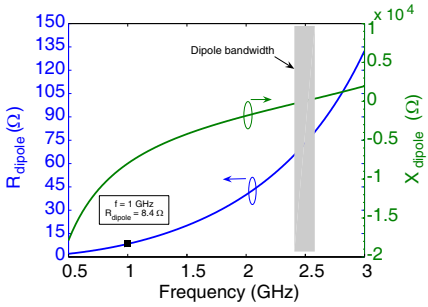

Figure 4. Dipole resistance and reactance for $l = 6\,\mathrm{cm}$ and $a = 0.1\,\mathrm{mm}$. The resonant frequency is $f_0 = 2.5\,\mathrm{GHz}$ and the dipole bandwidth is $f_0/10\,\mathrm{GHz}$, $R_{dipole} < 10\,\Omega$ for $f \leq 1\,\mathrm{GHz}$.

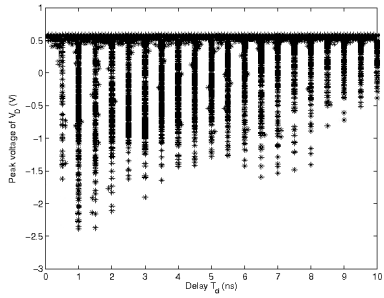

Figure 5. Bifurcation diagram using the parameter T_d with $Z_g = 5\,\Omega$ and $E_g = 2\,\mathrm{V}$.

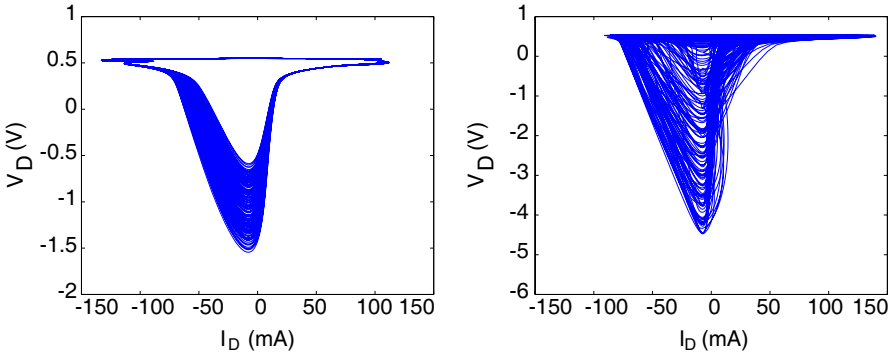

Figure 6. Attractors for $E_g = 2\,\mathrm{V}$ and $Z_g = 5\,\Omega$: (a) $T_d = 1.3\,\mathrm{ns}$, (b) $T_d = 1\,\mathrm{ns}$.

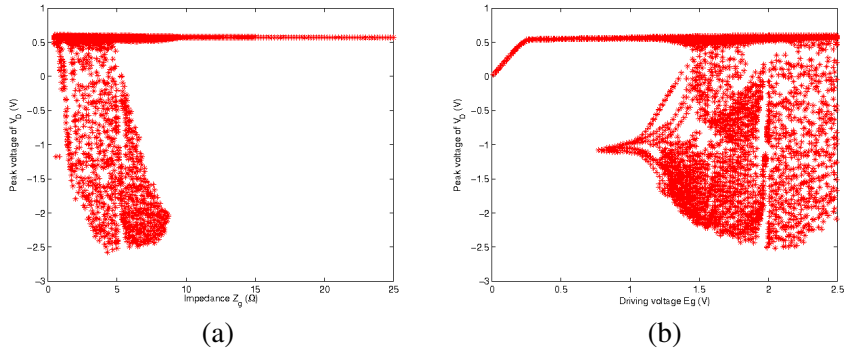

Figure 7. Bifurcation diagrams at $T_d = 1\,\mathrm{ns}$: (a) Bifurcation parameter Z_g at $E_g = 2\,\mathrm{V}$ and (b) bifurcation parameter E_g at $Z_g = 5\,\Omega$.

3. ELECTRICAL SIMULATIONS

The design of the studied limiter model of Figure 1 is analyzed with the microwave electrical software; "*Advanced Design System*" (*ADS*). The PIN diode is described by a complete model available in the *ADS* library. The electrical characteristics are the same as those of the theoretical result part. The Figure 7 depicts the bifurcation diagrams with the bifurcation parameters Z_g and E_g.

From the bifurcation diagrams, we plot the periodic and chaotic attractors for two different amplitudes of the driving source (Figure 8).

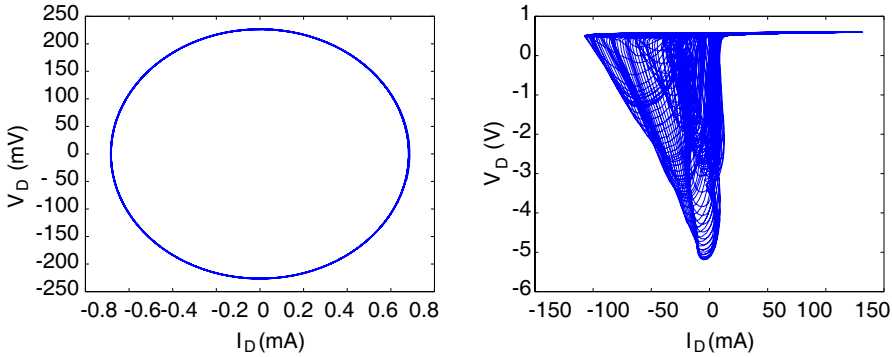

Figure 8. Attractors at $Z_g = 5\,\Omega$ and $T_d = 1\,\text{ns}$: (a) Periodic attractor for $E_g = 0.1\,\text{V}$ and (b) chaotic attractor for $E_g = 2\,\text{V}$.

We find a good agreement between the theoretical results and those obtained by using the electrical simulations. In the bifurcation diagrams, the borders between the periodic and chaotic operating regimes are similar with those given by the theoretical part, up to $Z_g = 8\,\Omega$ and for a minimum driving voltage $E_g = 1.4\,\text{V}$. The shapes and the amplitudes of attractors are also comparable. Compared to the simulation study, the theory allows to understand more precisely the parameters which govern the chaotic behavior. In the other hand, the simulations allow to validate the theory by using a complete model which accounts for the parasitic elements of the diode but necessitate the knowledge of theoretical conditions which ensure to obtain a chaotic behavior.

4. CONCLUSION

A delay nonlinear differential equation is proposed to understand the origin of the microwave chaotic behavior in the radar front-end limiter circuit. Bifurcation diagrams provide the conditions at which the chaotic behavior appears. They also show that the trajectory fills the phase space only for a periodic delay time of the half driving signal period. Simulation results agree well with the theoretical ones. This study can be extended to all the receiver systems where the protection circuits are needed. It can be also extended to the other cases where the line impedance is different of $50\,\Omega$.

ACKNOWLEDGMENT

This work which concerns a Ph.D. thesis is supported by the "DGA" ("Direction Générale de l'Armement") and the "CEA" ("Commissariat à l'Energie Atomique et aux Energies Alternatives").

REFERENCES

1. *The PIN Diode Circuit Designers' Handbook*, No. 98=WPD-RDJ007, Microsemi Corporation, Watertown, Santa Ana, California, DOC, 1998.
2. "Applications of PIN diodes," Application Note 922, Hewlett Packard, 2008.
3. Leenov, D., "The silicon PIN diode as a microwave radar protector at megawatt levels," *IEEE Trans. on Electron. Devices*, Vol. 4, No. 12, 53–61, 1964.
4. Glenn, C. M. and S. Hayes, "Observation of chaos in a microwave limiter circuit," *IEEE Microwave and Guided Wave Lett.*, Vol. 4, No. 12, 417–419, 1994.
5. Granatstein, V. L., et al., "Effects of hight power micro-waves and chaos in 21st century analog and digital electronics," *AFOSR, MURI*, No. F496200110374, Institute for Research in Electronics and Applied Physics, University of Maryland College Park, MD 20743-3511, 2006.
6. Blakely, J. N., J. D. Holder, N. J. Corron, and S. D. Pethel, "Simply folded band chaos in a VHF microstrip oscillator," *Phys. Lett.*, Vol. 346, No. 1–3, 111–114, 2005.
7. Caroll, T. L. and L. M. Pecora, "Parameter ranges for the onset of period doubling in the diode resonator," *Phys. Rev. E*, Vol. 66, 2002.
8. Su, Z., R. W. Rollins, and E. R. Hunt, "Simulation and characterization of strange attractors in driven diode resonator systems," *Phys. Rev. A*, Vol. 40, 1989.
9. Ma, C. L., P. O. Lauritzen, and J. Sigg, "Modeling of power diodes with the lumped-charge modeling technique," *IEEE Trans. on Power Electronics*, Vol. 12, No. 3, 398–405, 1997.
10. Drozdovskaia, L., "RF and microwave frequency properties of a reverse-biased thick switching P-I-N diode," *IEEE Trans. on Microwave Theory and Techniques*, Vol. 49, No. 8, 2001.
11. Strollo, A. G. M., "A new SPICE model of power P-I-N diode based on asymptotic waveform evaluation," *IEEE Trans. on Power Electronics*, Vol. 12, No. 1, 1997.

12. Sze, S. M., *Physics of Semiconductor Devices*, 2nd Edition, Wiley-Interscience, 1981.
13. "BAP64-02 silicon PIN diode," Data Sheet, No. 9397 750 06912, Philips Semiconductors, 2000.
14. Balanis, C. A., *Antenna Theory Analysis and Design*, Wiley-Interscience, New York, 2005.
15. Vittanen, A. J., "Radiation impedance of half wave length dipole antenna in terms of Bessel functions," *IEEE 10th Mediterranean Electrotechnical Conference, MEleCon2000*, Vol. 1, 2000.